PERGAMON

International Journal of Solids and Structures 40 (2003) 447–464

INTERNATIONAL JOURNAL OF SOLIDS and STRUCTURES

www.elsevier.com/locate/ijsolstr

# A simple method for calculating interaction of numerous microcracks and its applications

Xi-Qiao Feng *, Jia-Yin Li, Shou-Wen Yu

*Department of Engineering Mechanics, Tsinghua University, Beijing 100084, PR China*

Received 6 November 2001; received in revised form 12 August 2002

**Abstract**

The effects of microcrack interaction on the failure behavior of materials present one problem of considerable interest in micromechanics, which has been extensively argued but has not been resolved as yet. In the present paper, a simple and effective method is presented based on the concept of the effective field to analyze the interaction of microcracks of a large number or of a high density. To determine the stress intensity factors of a microcrack embedded in a solid containing numerous or even countless microcracks, the solid is divided into two regions. The interaction of microcracks in a circular or elliptical region around the considered microcrack is calculated directly by using Kachanov's micromechanics method, while the influence of all other microcracks is reflected by modifying the stress applied in the far field. Both the cases of tensile and compressive loading are considered. This simplified scheme may yield an estimate for stress intensity factors of satisfactory accuracy, and therefore provide a potential tool for elucidating some phenomena of material failure associated with microcracking. As two of its various promising applications, the above scheme is employed to investigate the size effects of material strength due to stochastic distribution of interacting microcracks and to calculate the effective elastic moduli of elastic solids containing distributed microcracks. Some conventional micromechanics methods for estimating the effective moduli of microcracked materials are evaluated by comparing with the numerical results. Only two-dimensional problems have been considered here, though the three-dimensional extension of the present method is of greater interest.


*Keywords:* Micromechanics; Non-homogeneous media; Elastic moduli; Microcrack interaction; Numerical methods; Stress intensity factor; Size effect

## 1. Introduction

Many phenomena of deformation and failure of brittle or quasi-brittle solids are associated with interaction and propagation of disordered microcracks. The problem of microcrack interaction has been extensively investigated over the past decades but has not been resolved yet. Such transport properties as

* Corresponding author. Tel.: +86-10-6277-2934; fax: +86-10-6278-1824.
*E-mail address:* fengxq@tsinghua.edu.cn (X.-Q. Feng).

0020-7683/02/$ - see front matter 
PII: S0020-7683(02)00519-X

the effective elastic moduli and thermal conductivities of microcracked solids are closely related to the statistically averaged, zeroth- and first-order effects of microcrack interaction. However, such failure-related properties as the load-bearing capacity and the strain-softening behavior are sensitive to the sizes, locations and orientations of individual microcracks, namely, higher-order effects of microcrack interaction. On one hand, therefore, some effective medium or effective field methods, e.g. the self-consistent method (SCM) (Budiansky and O'Connell, 1976; Horii and Nemat-Nasser, 1983), the generalized self-consistent method (GSCM) (Christensen and Lo, 1979; Huang et al., 1994, 1996), the differential method (DM) (Zimmerman, 1985; Hashin, 1988), Mori–Tanaka method (MTM) (Mori and Tanaka, 1973; Benveniste, 1986) and the interactive direct-derivation (IDD) method (Zheng and Du, 1997, 2001), have been established for estimating the impacts of microcrack interaction on the effective elastic moduli of microcracked solids (Kachanov, 1993; Krajcinovic, 1996; Feng and Yu, 2002). These methods, with few exceptions, omit the concrete positions and orientations of individual microcracks. To gain an insight into the failure behavior of brittle solids, on the other hand, direct interaction of microcracks has to be taken into account.

Micromechanical discrete methods and finite element analysis may provide the stress intensity factors (SIFs) of multiple interacting microcracks of a specified array. Owing to the difficulty in obtaining an analytical solution of such problems, some approximate numerical schemes have been developed. Among them, several typical examples are the method of pseudo-tractions (Hori and Nemat-Nasser, 1987; Kachanov, 1987), the complex potential method (Gong and Horii, 1989), the double potential method (Chudnovsky et al., 1987), and the weight function method (Bueckner, 1975). Literature reviews on the calculation of microcrack interaction have been given by Karihaloo (1979), Kachanov (1993), Chen (1995), Feng and Yu (2002), Petrova et al. (2000), and many others. The problem of interaction of multiple microcracks is often reduced to a set of integral equations, which can be solved by the series expansion method, perturbation method, boundary element method, collocation method, and some other approximate methods. In addition, actual problems of crack interaction are generally three-dimensional (3D), but due to the complexity of calculation, most investigations on this subject are still limited to two-dimensional (2D) crack arrays.

Theoretically, the above mentioned methods can be used in the case of numerous microcracks. However, the number of equations increases very rapidly with the increase in the number of microcracks. The cumbersome numerical computation limits the application of these methods to only those situations where the number of microcracks is relatively small (see, e.g., Kachanov, 1987, 1993; Huang et al., 1994, 1996; Zhan et al., 1999; Seelig et al., 2000; Shen and Yi, 2001). To date, there seems to be no method yet available for calculating the interaction of microcracks of a large number, as in most cases of actual materials. It seems straightforward to calculate the SIFs of a microcrack by considering merely its neighboring microcracks and omitting those far from it. Unfortunately, such a simplification is inappropriate, especially in the case of higher concentration of microcracks, as will be illustrated in the next section.

Therefore, an attempt is made in this paper to present a novel method to calculate the interaction of numerous disordered microcracks. Recently, Zheng and Du (1997, 2001) developed the IDD method for estimating the elastic moduli of heterogeneous materials with microdefect interaction effects in a skillful and effective manner. Feng (2001) elucidated the correspondence relation between the effective medium method and the effective field method in estimation of elastic moduli. Combining Kachanov's method for calculating the direct interaction of microcracks in a local region with the concept of the effective stress field in the global sense, a simple method is suggested in the present paper for analyzing the strong interaction of distributed microcracks of a large number. Both the cases of tension and compression are considered. To illustrate its various applications, this global/local method is used to examine the size effects of material strength and to calculate the effective elastic moduli of microcrack-weakened materials.

## 2. Effective field-subregion model

### 2.1. Model

Consider a plate $S$ subjected to a uniform stress $\boldsymbol{\sigma}_\infty$ in the far field and weakened by a large number of statistically distributed, planar microcracks, as shown in Fig. 1(a). First, let us consider a microcrack in it, say the $\alpha$th one, whose length is denoted as $2l_\alpha$. Refer to a global Cartesian coordinate system $(O-x_1x_2)$ and a local system $(O-x_1'x_2')$ with the $x_2'$-axis aligned with the normal $\mathbf{n}^\alpha$ of this microcrack, as shown in Fig. 2. The microcrack orientation is then expressible in terms of an angle, $\theta_\alpha$. Assume that the statistical distribution of the orientations and sizes of all microcracks satisfies a probability density distribution function, $p(l,\theta)$.

It is very difficult or even impossible to calculate the exact SIFs of the $\alpha$th microcrack, which interacts with all the other, numerous or even countless, microcracks. Therefore, some approximations or simplifications are necessary even when numerical methods are adopted. Evidently, the local stress fields around the $\alpha$th microcrack are sensitive to the positions, orientations and sizes of the neighboring microcracks around it. In fact, it is generally unnecessary and meaningless to calculate directly the weak interaction between two microcracks if they are very far from each other in such a microcrack-profuse solid. In the present approximate scheme, therefore, a subregion $\Omega$ of the plate is defined around the $\alpha$th microcrack, as schematized in Fig. 1(b). The size of $\Omega$ is much larger than that of a single microcrack, e.g., 10 or 20 times the average length of microcracks, while the shape of $\Omega$ may be specified according to the statistical distribution of microcrack orientations. An elliptical shape can generally be specified with its two principal axes $2a_1$ and $2a_2$ aligned with the $x_1$- and $x_2$-directions, respectively, as shown in Fig. 1(b). In the isotropic

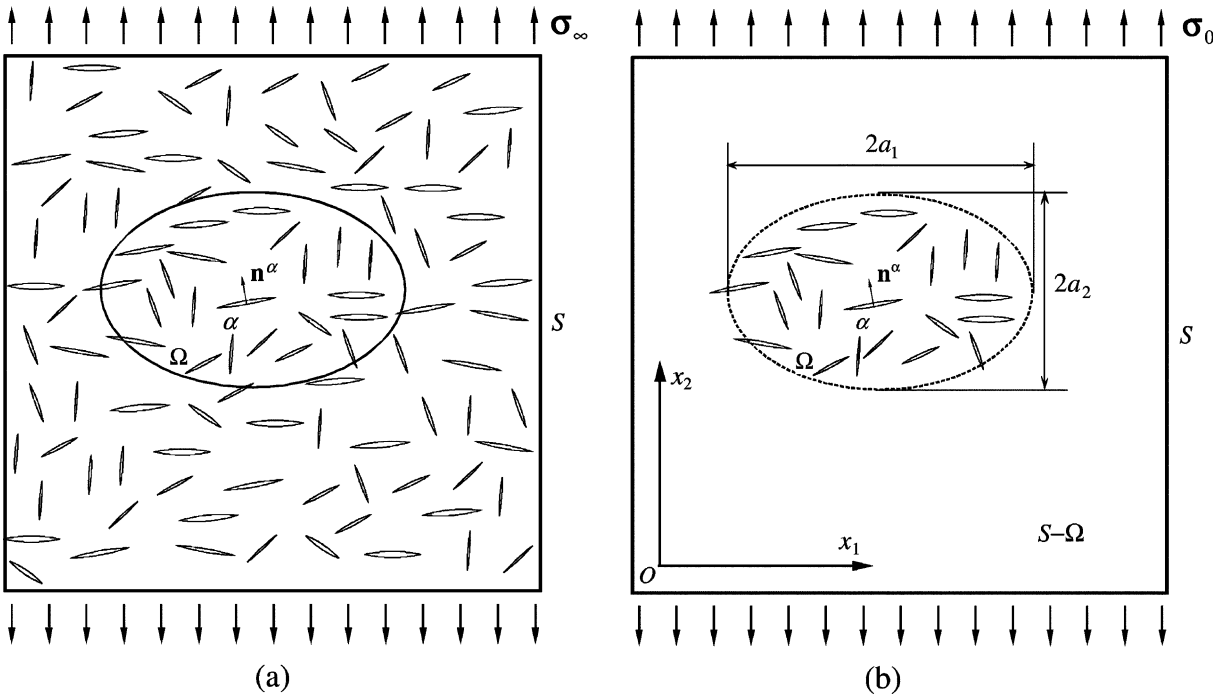


Fig. 1. (a) An elastic matrix containing distributed microcracks, and (b) the approximate model for calculating the SIFs of the $\alpha$th microcrack.

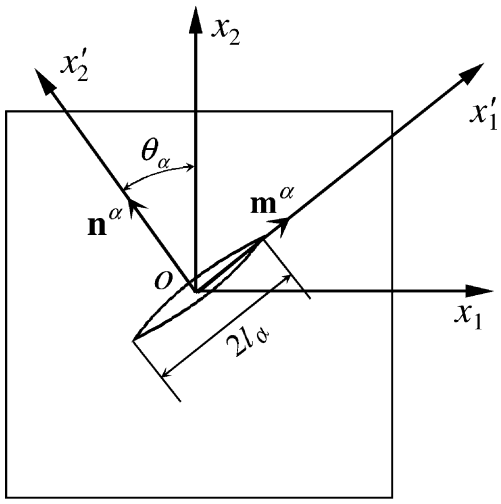


Fig. 2. Global and local coordinate systems.

case of completely random orientations, it is reasonable and convenient to choose $\Omega$ of circular shape. More detailed discussion on the specification of the shape and size of $\Omega$ will be made in the sequel based on numerical examples.

The interaction of those microcracks with centers located in $\Omega$ may be calculated by one of the various micromechanical methods mentioned in the introduction. However, it is conceptually inappropriate to neglect completely the microcracks out of $\Omega$, even though the size of $\Omega$ is much larger than the characteristic size of microcracks. The subregion $\Omega$ exists in the plate as a weakened "inclusion" with an effective elastic stiffness lower than that of the pristine matrix. Neglecting all the microcracks outside $\Omega$ renders the outside medium stiffer than the actual microcracked plate, and therefore leads to an incorrect result that the average stress $\boldsymbol{\sigma}_\Omega$ within $\Omega$ is lower than the far-field stress $\boldsymbol{\sigma}_\infty$. In other words, although the interaction between the $\alpha$th microcrack and a single microcrack in $S-\Omega$ is weak, the total contribution of all the numerous microcracks in $S-\Omega$ to the SIFs of the $\alpha$th microcrack is finite and, generally, should be taken into consideration. Therefore, a modified far-field stress $\boldsymbol{\sigma}_0$ is applied in the approximate model in Fig. 1(b) such that the average stress within the region $\Omega$ remains the correct value, $\boldsymbol{\sigma}_\infty$.

According to the well-known Eshelby's theory, the stress and strain fields in an elliptical inclusion embedded in an otherwise homogeneous infinite matrix are uniform when a constant stress is applied in the far field. Accordingly, the average stress within the inclusion $\Omega$ in Fig. 1(b) is expressed as (Mura, 1987)

$$\boldsymbol{\sigma}_\Omega = \mathbf{B} : \boldsymbol{\sigma}_0. \tag{1}$$

The fourth-order tensor $\mathbf{B}$, which is referred to as the average stress concentration tensor in the literature, was expressed by Walpole (1969) as

$$\mathbf{B} = [\mathbf{I} + \mathbf{P} : (\mathbf{M} - \mathbf{M}_0)]^{-1}, \tag{2}$$

where $\mathbf{M}_0$ and $\mathbf{M}$ denote the elastic compliance tensors of the pristine matrix and the microcracked inclusion $\Omega$, respectively, and $\mathbf{I}$ is the fourth-order unit tensor. Throughout this paper, a boldface letter stands for a vector or tensor, and a colon between two tensors denotes contraction (inner product) over two indices. The fourth-order tensor $\mathbf{P}$ in Eq. (2) is related to Eshelby's tensor $\mathbf{S}$ by

$$\mathbf{P} = \mathbf{L}_0 : (\mathbf{I} - \mathbf{S}), \tag{3}$$

where $\mathbf{L}_0 = \mathbf{M}_0^{-1}$ is the elastic stiffness tensor of the matrix. Therefore, $\mathbf{P}$ depends on the orientation and shape of the inclusion as well as on the elastic moduli of the surrounding matrix. Some analytical expressions of $\mathbf{S}$ and $\mathbf{B}$ can be found in the literature (see, e.g., Walpole, 1969; Mura, 1987).

It is easily proved that in the case of a uniform traction boundary condition, the presence of microcracks does not change the average stress within the material (Kachanov, 1993). This means that if all the microcracks both outside and inside the region $\Omega$ were considered, the average stress in $\Omega$ would equal approximately to the far-field stress, $\boldsymbol{\sigma}_\infty$. To yield an exact estimate of the SIFs of the $\alpha$th microcrack from the approximate model in Fig. 1(b), therefore, one should have

$$\boldsymbol{\sigma}_\Omega = \boldsymbol{\sigma}_\infty. \tag{4}$$

From Eqs. (1) and (4), the modified far-field stress in Fig. 1(b) should be

$$\boldsymbol{\sigma}_0 = \mathbf{B}^{-1} : \boldsymbol{\sigma}_\infty. \tag{5}$$

Thus in the present method, the microcracks throughout the plate $S$ are divided into two groups, which are treated in different ways in calculation of their contributions to the SIFs of the $\alpha$th microcrack. The interacting microcracks inside $\Omega$ are calculated directly from a discrete micromechanical method, while the influence of those cracks out of $\Omega$ is reflected by modifying the far-field stress. Some further details of this global/local model will be discussed in the following sections of this chapter, including the estimation of the effective elastic moduli $\mathbf{M}$, the calculation of the direct interaction of microcracks in $\Omega$, and the determination of the shape and size of $\Omega$.

By the way, only the case of a traction boundary condition on the microcracked specimen is considered in this paper because that of displacement boundary condition can be studied analogously. For the latter case, the average strain tensor compatible to the given displacements in the far field should be modified in terms of the average strain concentration tensor.

### 2.2. Effective moduli of microcracked solids

To determine the stress concentration tensor $\mathbf{B}$ in Eq. (5), the effective compliance tensor $\mathbf{M}$ in Eq. (2) of the microcracked inclusion $\Omega$ has to be determined first. Among the effective medium methods aforementioned, the non-interacting approximation and the SCM provide an upper bound and a lower bound of the effective stiffness tensor, respectively. A more exact result can be obtained from the Taylor model-based effective medium method, which was recently suggested by Feng and Yu (2000) and will be adopted in the present paper, though other methods (e.g., the DM and IDD method) are also applicable.

An isotropic plate weakened by numerous microcracks of uniformly random locations and orientations is first taken as an illustration. In this case, as discussed above, the subregion $\Omega$ is specified as a circular shape. For convenience in formulation, we express a 2D symmetric fourth-order tensor in the form of $3 \times 3$ matrix by using the abbreviated notations 1, 2 and 3 for 11, 22 and 12 (or 21), respectively. Then, the compliance tensor of the isotropic matrix with Young's modulus $E_0$ and Poisson's ratio $v_0$ is expressed as

$$[\mathbf{M}_0] = \frac{1}{E_0}\begin{bmatrix} 1 & -v_0 & 0 \\ -v_0 & 1 & 0 \\ 0 & 0 & 1+v_0 \end{bmatrix}. \tag{6}$$

For a circular inclusion embedded in such a matrix, we have (Mura, 1987):

$$[\mathbf{P}] = \frac{E_0}{4}\begin{bmatrix} 3/2 & 1/2 & 0 \\ 1/2 & 3/2 & 0 \\ 0 & 0 & 1 \end{bmatrix}. \tag{7}$$

Then using the method of Feng and Yu (2000), the effective compliance tensor of an elastic solid containing randomly oriented microcracks is expressed as

$$[\mathbf{M}] = \frac{1}{E}\begin{bmatrix} 1 & -v & 0 \\ -v & 1 & 0 \\ 0 & 0 & 1+v \end{bmatrix}, \tag{8}$$

with the effective Young's modulus and Poisson's ratio being given by

$$E = E_0[1+\pi\omega(1+\pi\omega)]^{-1}, \quad v = v_0[1+\pi\omega(1+\pi\omega)]^{-1}, \tag{9}$$

respectively, where $\omega = (1/A)\sum_{\alpha=1}^{N}(l_\alpha)^2$ is the conventional 2D scalar microcrack density parameter (Bristow, 1960), $A$ the area of $\Omega$, and $N$ the number of microcracks in $\Omega$.

In another extreme case where all microcracks are aligned along the direction of the $x_1$-axis, the effective compliance tensor of $\Omega$ is obtained from the same method as (Feng and Yu, 2000)

$$[\mathbf{M}] = \begin{bmatrix} 1/E_{11} & -v_{12}/E_{11} & 0 \\ -v_{12}/E_{11} & 1/E_{22} & 0 \\ 0 & 0 & 1/(2G_{12}) \end{bmatrix}, \tag{10}$$

where

$$\begin{aligned} E_{11} &= E_0, \quad v_{12} = v_0, \\ E_{22} &= E_0\left\{1+\pi\omega\sqrt{2+4\pi\omega}\left[1+2\pi\omega(1+v_0)+\sqrt{1+2\pi\omega}\right]^{1/2}\right\}^{-1}, \\ G_{12} &= G_0\left\{1+\frac{\sqrt{2}\pi\omega}{2(1+v_0)}\left[1+2\pi\omega(1+v_0)+\sqrt{1+2\pi\omega}\right]^{1/2}\right\}^{-1}, \end{aligned} \tag{11}$$

with $G_0 = E_0/(2(1+v_0))$ being the shear modulus of the matrix.

### 2.3. Stress intensity factors of interacting microcracks

Kachanov's method of microcrack interaction (Kachanov, 1987, 1993) is employed in the present paper owing to its simplicity and effectiveness in most cases of microcrack array and density. This method is reviewed briefly in the Appendix A. Thereby, the SIFs at the tips of the $\alpha$th microcrack can be calculated by (Tada, 1973)

$$\begin{aligned} K_{\mathrm{I}}^{\alpha}(\pm l_\alpha) &= \frac{1}{\sqrt{\pi l_\alpha}}\int_{-l_\alpha}^{l_\alpha}\sqrt{\frac{l_\alpha \pm \xi}{l_\alpha \mp \xi}}p^{\alpha}(\xi)\,\mathrm{d}\xi, \\ K_{\mathrm{II}}^{\alpha}(\pm l_\alpha) &= \frac{1}{\sqrt{\pi l_\alpha}}\int_{-l_\alpha}^{l_\alpha}\sqrt{\frac{l_\alpha \pm \xi}{l_\alpha \mp \xi}}\tau^{\alpha}(\xi)\,\mathrm{d}\xi, \end{aligned} \tag{12}$$

where $p^{\alpha}(\xi)$ and $\tau^{\alpha}(\xi)$ denote, respectively, the normal and tangential pseudo-tractions at position $\xi$ along the $\alpha$th crack, and $\xi = \pm l_\alpha$ corresponds to the two tips of the crack.

### 2.4. Shape and size of subregion $\Omega$

To reveal some basic aspects of the presented method, two examples are considered in this section for calculation of the SIFs of a microcrack interacting with many others.

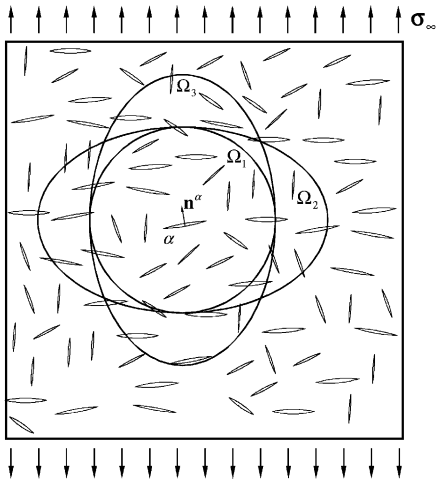


Fig. 3. Definition of the subregion $\Omega$ in the case of randomly oriented microcracks.

*2.4.1. Case 1: randomly oriented microcracks*

Consider first an isotropic plate with numerous microcracks of completely random locations and orientations, as shown in Fig. 3. The density of microcracks is taken as $n_c = 2500\ \mathrm{m}^{-2}$. Their half-lengths satisfy a normal distribution law $\Phi(l)$ with the mathematical expectation value being 5 mm and the variance being 1 mm. A uniaxial tensile stress is applied in the direction of $x_2$-axis, that is, $\sigma_{22}^{\infty} = \sigma^{\infty} > 0$ and $\sigma_{ij}^{\infty} = 0$ for other $i$ and $j$.

The effect of the shape of the subregion $\Omega$ on the SIFs of a microcrack is examined first. An elliptical shape is specified for the region $\Omega$. Different aspect ratios $a_1/a_2$ of $\Omega$ are analyzed while keeping the minor half-axis, $a_{\min} = \min[a_1, a_2]$, being a constant value. Three such subregions are schematized in Fig. 3 to calculate the SIFs of the $\alpha$th microcrack. It is found from a sufficient number of numerical examples that the shape of $\Omega$ exerts little influence on the SIFs provided that $a_{\min}$ is large enough. This implies that in the isotropic case, the circular shape (i.e., $a_1 = a_2 = a$) should be chosen for $\Omega$, which contains the least number of microcracks making the calculation easier.

Then the influence of the size of $\Omega$ is investigated. The numerical results show that the SIFs of a microcrack possess a pronounced dispersion when the radius $a$ of $\Omega$ is small (e.g. three times the average half-length of microcracks). This reflects the strong interaction of microcracks that are close to each other, and indicates the necessity to account for direct interaction in analysis of failure behavior of brittle solids. The SIFs of the microcrack approach to stable values when $a$ is much larger than the characteristic size of microcracks. A further increase in the size of $\Omega$ does not cause evident change in the SIFs of the microcrack. Therefore, it is unnecessary to calculate the direct interaction of microcracks that are far from each other. However, a large size of $\Omega$ will certainly lead to a cumbersome calculation, especially when the SIFs of many microcracks need to be determined. According to our numerical analysis, a value of $a$ between 10 and 20 times the average half-length of microcracks seems suitable to achieve a balance of the accuracy of results and the simplicity of calculation. One may decide the dimension of a subregion by considering such factors as the microcrack density and the required accuracy. For a high microcrack density, a relatively small subregion may be defined to yield an easier calculation. An empirical criterion is that a region containing about 100 microcracks will be large enough to yield a satisfactory accuracy and small enough to calculate easily. In addition, the numerical results also prove that the cracks in the complementary region $S - \Omega$ has an evident influence on the SIFs of a crack in $\Omega$, especially when the crack concentration is high.

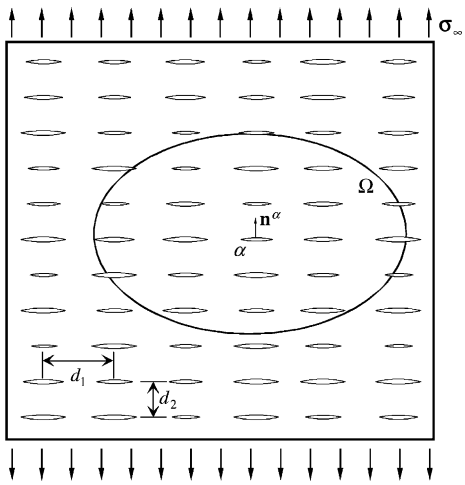


Fig. 4. Definition of the subregion $\Omega$ in the case of parallel microcracks.

*2.4.2. Case 2: parallel microcracks*

In this example, we consider a plate with a family of parallel microcracks normal to the $x_2$-axis. Their centers are located in a regular and doubly periodic manner, as shown in Fig. 4, where $d_1$ and $d_2$ denote the spacings of neighboring cracks in the $x_1$- and $x_2$-directions. Their lengths satisfy the same normal distribution rule as in the first example. A uniaxial tensile stress $\sigma_{22}^{\infty} = \sigma^{\infty}$ is assumed. The analysis on the effects of the shape and size of $\Omega$ yields similar conclusions as those in the first example, except that an elliptic shape of $\Omega$ seems more appropriate when the difference between $d_1$ and $d_2$ is relatively large.

## 3. Size effect under tension

It is well known that the strength of specimens of a brittle or quasi-brittle material usually exhibits a significant size effect. That is, the material strength measured decreases evidently as the specimen size increases. This size effect of such engineering brittle materials as concrete and rocks are caused mainly by their heterogeneous microstructures due to the stochastic distribution of constituent phases and microdefects. Using the effective field-subregion method presented above, the size effect of material strength associated with interacting microcracks is examined here for otherwise homogeneous brittle solids.

2D rectangular plate specimens with length $2L$ and width $L$ are taken as an example, as shown in Fig. 5(a). The boundary effect is disregarded in this paper, because the size of specimens is assumed much larger than the average length of microcracks. In such a case, the interaction of disordered microcracks is the main reason for the size effect of specimen strength. According to the effective field-subregion method, only when a microcrack is far from the boundary of a subregion $\Omega$, can its stress intensity factors be calculated exactly. Therefore, a sufficient large number of subregions are chosen such that each microcrack is near the center of a subregion.

For a mixed-mode crack in a brittle solid, the energy release rate theory developed initially by Griffith is often taken as the controlling parameter of crack growth. Accordingly, the mixed-mode fracture criterion may be written as (Kanninen and Popelar, 1985; Feng and Yu, 2002)

$$G = \left(\frac{K_{\mathrm{I}}}{K_{\mathrm{IC}}}\right)^2 + \left(\frac{K_{\mathrm{II}}}{K_{\mathrm{IIC}}}\right)^2 = 1, \tag{13}$$

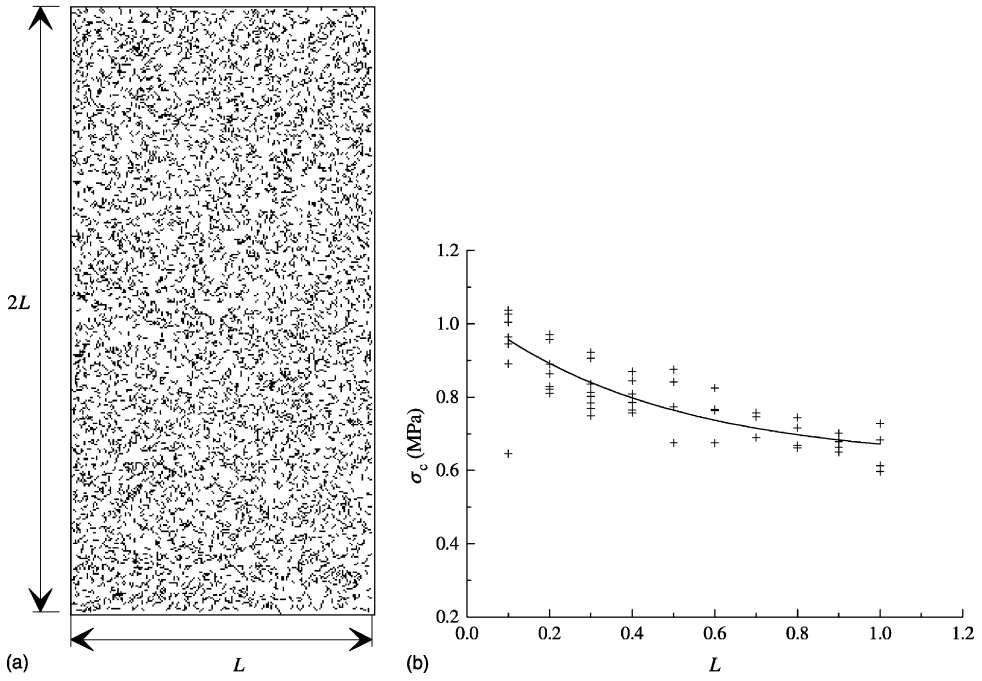


Fig. 5. (a) A specimen with randomly orientated microcracks, and (b) the size effect of specimen strength under tension.

where $K_{\mathrm{I}}$ and $K_{\mathrm{II}}$ represent the mode-I and II SIFs, $K_{\mathrm{IC}}$ and $K_{\mathrm{IIC}}$ their intrinsic critical values, respectively. For simplicity, $K_{\mathrm{IC}}$ and $K_{\mathrm{IIC}}$ are regarded as material constants without dependence upon microcrack propagation. This is exact only for perfectly brittle materials, in which the release of internal energy due to microcrack growth is entirely transformed into the increase in the surface energy of propagated microcracks, that is, no other microscopic dissipation mechanism exists at crack tips. For actual materials, $K_{\mathrm{IC}}$ and $K_{\mathrm{IIC}}$ generally increase as a crack grows. This will weaken the size effect of material strength but is not considered in the present paper. To emphasize the effect of microcrack interaction, furthermore, we assume that $K_{\mathrm{IC}}$ and $K_{\mathrm{IIC}}$ are spatially uniform. For a heterogeneous matrix as in most actual materials, the spatial fluctuation of $K_{\mathrm{IC}}$ and $K_{\mathrm{IIC}}$ can easily be accounted for in the present method by specifying different values of $K_{\mathrm{IC}}$ and $K_{\mathrm{IIC}}$ for different microcracks.

To determine the load-bearing capacity of a specimen, the far-field stress is denoted as $\boldsymbol{\sigma}_\infty = m\boldsymbol{\sigma}^0_\infty$, where $\boldsymbol{\sigma}^0_\infty$ is a reference stress tensor and $m$ is a load factor. The mode-I and II SIFs at the two tips of the $\alpha$th microcrack subjected to the reference stress $\boldsymbol{\sigma}^0_\infty$ are calculated by using the method in Section 2 and designated as $K^\alpha_{\mathrm{I}0}(\pm l_\alpha)$ and $K^\alpha_{\mathrm{II}0}(\pm l_\alpha)$, respectively. Thus, the $\alpha$th microcrack will undergo an unstable propagation at one of its two tips when the load factor $m$ reaches the following value:

$$m_\alpha = \min\left\{\left[\left(\frac{K^\alpha_{\mathrm{I}0}(l_\alpha)}{K_{\mathrm{IC}}}\right)^2 + \left(\frac{K^\alpha_{\mathrm{II}0}(l_\alpha)}{K_{\mathrm{IIC}}}\right)^2\right]^{-1/2}, \quad \left[\left(\frac{K^\alpha_{\mathrm{I}0}(-l_\alpha)}{K_{\mathrm{IC}}}\right)^2 + \left(\frac{K^\alpha_{\mathrm{II}0}(-l_\alpha)}{K_{\mathrm{IIC}}}\right)^2\right]^{-1/2}\right\}. \tag{14}$$

The specimen strength is defined as the applied stress $\boldsymbol{\sigma}_{\mathrm{c}}$ at which any one of the microcracks starts to propagate. That is,

$$\boldsymbol{\sigma}_{\mathrm{c}} = m_{\mathrm{c}}\boldsymbol{\sigma}^0_\infty, \tag{15}$$

where the critical load factor $m_c$ is the minimum value of $m_\alpha$ among all the microcracks:

$$m_c = \min\{m_\alpha,\ \alpha = 1, 2, \ldots, N\}. \tag{16}$$

For instance, consider rectangular specimens with length $2L$ and width $L$, subjected to uniaxial tension in the $x_2$-direction. Take the following material parameters for the matrix: the Young's modulus $E = 0.35 \times 10^5$ MPa, the Poisson's ratio $v = 0.3$, the critical SIFs $K_{IC} = 0.165$ MPa m$^{1/2}$ and $K_{IIC} = 0.330$ MPa m$^{1/2}$, and the number density of microcracks $n_c = 2500$ m$^{-2}$. The sizes of microcracks satisfy the same normal distribution law $\Phi(l)$ as in Section 2.4.

The orientations, sizes and locations of microcracks in each sample of specimens are specified by a computer program according to their probabilistic density distribution functions. Several samples of the same size are randomly produced, and their strengths are calculated respectively. Specimens of different sizes are considered by varying the parameter $L$ in order to verify the size effect of strength. Each specimen may contain microcracks of a great number, say, 5000. If the direct interaction of all these microcracks is calculated, one has to solve a system of 10 000 equations, each of which has interactive terms (or transmission $\Lambda$-factors) of a very large number (about $1.2 \times 10^7$). Evidently, such a calculation is very difficult, and, in fact, it is also unnecessary. By using our present method, however, if a subregion contains 100 microcracks, one needs to solve only a system of 200 equations, each having less than 5000 interactive terms. As the total number of microcracks increases, the computation time increases proportionally, instead of exponentially.

Two cases of orientation distribution of microcracks are considered. In the first case, all microcracks are uniformly randomly oriented (Fig. 5(a)). The fracture stress averaged from multiple samples of the same size is plotted in Fig. 5(b) as a function of the specimen size. In the second case, all microcracks are aligned along the $x_1$-axis (Fig. 6(a)). The corresponding changing curve of the critical stress with respect to the specimen size is shown in Fig. 6(b). In both the cases, significant size effects of material strength have been

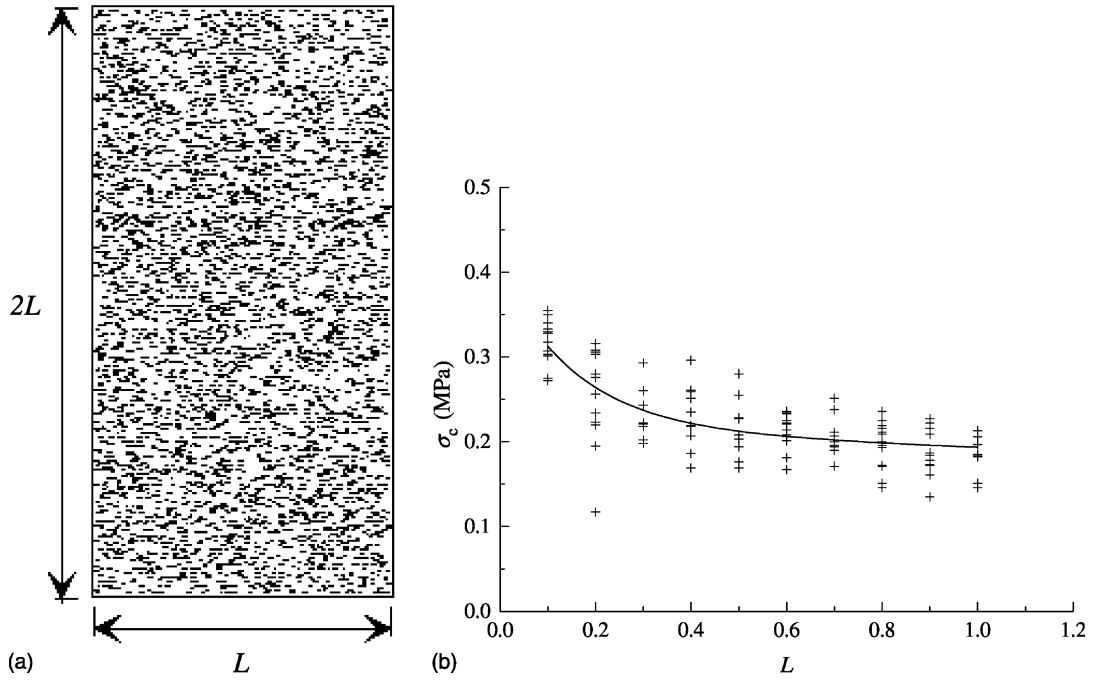


Fig. 6. (a) A specimen with parallel microcracks, and (b) the size effect of specimen strength under tension.

observed. The dispersion of the calculation results in the case of parallel microcracks is more pronounced than that of randomly oriented microcracks. This is physically reasonable because aligned microcracks are easier to coalesce than randomly orientated microcracks, or in other words, the interaction of aligned microcracks is stronger. It is seen that the particular statistics of microcracks dictates the failure and the associated size effect of brittle solids. The critical condition may fluctuate significantly depending upon the actual arrangement of the crack array.

It is also found from numerical calculations that as a consequence of interaction, a minority of microcracks are closed when a uniaxial tensile stress is applied. Interaction of closed microcracks can be considered in the calculation, as will be shown in the next section. However, no observable influence of closed microcracks has been found in our numerical results on the tensile strength of specimens. This is also reasonable because the load-bearing capacity of a brittle material exposed to tension is associated mainly with the fracture of open microcracks. Therefore, closed microcracks are assumed to be inactive, and their effect is negligible in the case of tension.

## 4. Size effect under compression

In this section, the size effect of material strength caused by microcrack interaction is further studied in the case of compression. Investigations on interaction of closed microcracks are still very limited. Basista and Gross (2000) extended Kachanov's method to 2D crack interaction problems under compression. Lehner and Kachanov (1995) analyzed the influence of interaction of frictional cracks on the stress-strain relations for rocks in compression. Carpinteri et al. (1996) studied the size effects of strength of brittle materials under compression using the boundary element method, including the coupling influences of crack interaction, propagation and intersection. However, only a small number of cracks can be considered by their method due to the cumbersome computation.

The effective field-subregion method presented in Section 2 can readily be extended to the case of compression by considering the following aspects in calculation:

(i) the closure and frictional sliding of microcracks,
(ii) the effective elastic moduli **M** of the microcracked solid and the stress concentration tensor **B**, which are different than those of tension, and
(iii) the fracture criterion of closed microcracks.

In the case of compression, the pseudo-tractions between the faces of a microcrack include three parts, namely, the tractions induced by the far-field stress, their fluctuations due to microcrack interaction, and the frictional forces. Thus, the normal and tangential tractions of the $\alpha$th microcrack are expressed as

$$\begin{aligned} p^{\alpha}(\xi) &= p^{\alpha}_{\infty} + \mathbf{n}^{\alpha} \cdot \sum_{\beta \neq \alpha} [\langle \tau^{\beta} \rangle \boldsymbol{\sigma}^{\alpha\beta}_{\tau}(\xi)] \cdot \mathbf{n}^{\alpha}, \\ \tau^{\alpha}(\xi) &= \tau^{\alpha}_{\infty} + \mathbf{n}^{\alpha} \cdot \sum_{\beta \neq \alpha} [\langle \tau^{\beta} \rangle \boldsymbol{\sigma}^{\alpha\beta}_{\tau}(\xi)] \cdot \mathbf{m}^{\alpha} - f^{\alpha}(\xi), \end{aligned} \tag{17}$$

respectively, where $\boldsymbol{\sigma}^{\alpha\beta}_{\tau}(\xi)$ denotes the induced stress at point $\xi$ of the $\alpha$th microcrack when a uniform tangential traction of unit intensity is loaded along the $\beta$th microcrack. The angle brackets stand for the average of a variable over the crack face.

The maximum frictional traction between the faces of the $\alpha$th microcrack is given by the Amontons frictional law:

$$f^{\alpha}_{\max} = \mu \langle p^{\alpha} \rangle, \tag{18}$$

where $\mu$ is the frictional coefficient. The driving force of frictional sliding is approximately expressed as

$$\langle \tau^{\alpha} \rangle_{\mathrm{d}} = \tau^{\alpha}_{\infty} + \mathbf{n}^{\alpha} \cdot \sum_{\beta \neq \alpha} [\langle \tau^{\beta} \rangle \boldsymbol{\sigma}^{\alpha\beta}_{\tau}(\xi)] \cdot \mathbf{m}^{\alpha}. \tag{19}$$

If the driving shear traction $\langle \tau^{\alpha} \rangle_{\mathrm{d}}$ is lower than the maximum frictional traction $f^{\alpha}_{\max}$, then there is no relative displacement between the two surfaces of the $\alpha$th microcrack, that is, this microcrack is inactive and makes no contribution to the SIFs of other microcracks. Frictional sliding occurs in the $\alpha$th microcrack when the average shear traction $\langle \tau^{\alpha} \rangle_{\mathrm{d}}$ reaches $f^{\alpha}_{\max}$.

In the case of uniaxial compression in the $x_2$-direction, frictional sliding occurs in the microcracks with orientations in the following range:

$$\theta_{\mathrm{f}} \leqslant \theta \leqslant \frac{\pi}{2}, \tag{20}$$

with $\theta_{\mathrm{f}} = \tan^{-1} \mu$, and all other microcracks are inactive. Then following the calculation scheme for closed microcracks in Yu and Feng (1995), the effective Young's modulus $E$ and Poisson's ratio $v$ under uniaxial compression are obtained readily as

$$\begin{aligned} E &= E_0 \left[ 1 + \frac{1}{3} n_{\mathrm{c}} a^2 (1 - \sin^3 \theta_{\mathrm{f}} - \mu \cos^3 \theta_{\mathrm{f}}) \right]^{-1}, \\ v &= \frac{E}{E_0} \left[ v_0 + \frac{1}{3} n_{\mathrm{c}} a^2 (1 - \sin^3 \theta_{\mathrm{f}} - \mu \cos^3 \theta_{\mathrm{f}}) \right]. \end{aligned} \tag{21}$$

Then the stress concentration tensor **B** can be determined from Eq. (2) in conjunction with (4) and (21). It should be noted that the effective elastic moduli in Eq. (21) and the corresponding **B** tensor can be used only in the case of uniaxial compression, because they are not constants but depend on the compressive stress state.

For a closed microcrack, $K_{\mathrm{I}} = 0$ and then the following fracture criterion is adopted:

$$K_{\mathrm{II}} = K_{\mathrm{IIC}}. \tag{22}$$

Similarly to Section 3, the far-field stress is expressed as $-\boldsymbol{\sigma}_{\infty} = -m\boldsymbol{\sigma}^{0}_{\infty}$, where $-\boldsymbol{\sigma}^{0}_{\infty}$ is a reference stress tensor and $m$ is a non-dimensional load factor. The critical load factor $m_{\mathrm{c}}$ is also defined as that when the first microcrack propagation occurs.

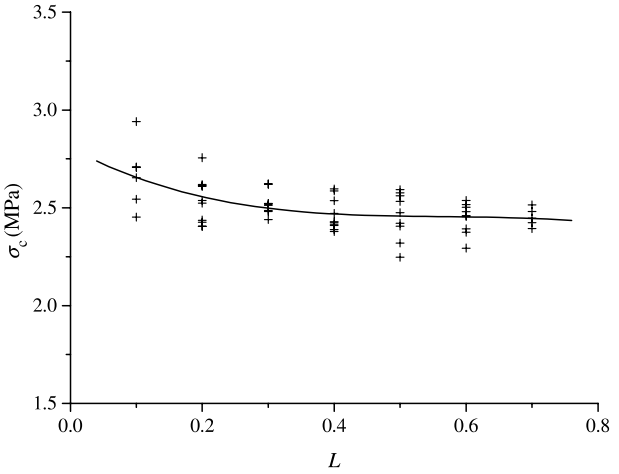


Fig. 7. The size effect of material strength under compression.

Consider again rectangular specimens of length $2L$ and width $L$, subjected to uniaxial compression in the $x_2$-direction. The material constants of the matrix are taken the same as those in Section 3. The frictional coefficient is taken as $\mu = 0.12$, and the number density of microcracks $n_c = 1225\ \mathrm{m}^{-2}$. Their sizes satisfy the same normal distribution as that in Section 3. It is found that due to interaction, some microcracks are open in the case of uniaxial compression. They are also considered in our calculation by using the method in Section 3. In the case of uniformly random orientation of microcracks, the dependence of the material strength on the specimen size is shown in Fig. 7. It is evident that the size effect in compression is less pronounced than that in tension. This is because some microcracks become inactive and the microcrack interaction is weakened due to friction. Again, it is found that the failure and the associated size effect of a brittle solid depend strongly on the statistics of microcracks.

## 5. Numerical calculation for effective elastic moduli of microcracked solids

As mentioned in the introduction, various micromechanics schemes have been established for estimating the effective moduli of an elastic matrix containing many dispersed microcracks. Such methods as the SCM, the GSCM, the DM, the MTM and the IDD method have been well reviewed and recapitulated by Kachanov (1993), Nemat-Nasser and Hori (1993), Krajcinovic (1996), Yu and Feng (1997), Zheng and Du (2001), and many others. To date, however, estimation of effective elastic moduli of microcracked solids is still a problem of extensive arguments. On one hand, the accuracy and the validation scopes of these established methods are yet to be evaluated further, and then it seems still a puzzling issue to determine which method should be employed for a specific problem. On the other hand, there is a lack of experimental data (Carvalho and Labuz, 1996) available in the literature for effective moduli of microcracked solids, especially for those with high concentration of microcracks. Therefore, it seems a promising approach to evaluate the accuracy of these micromechanics schemes via numerical methods. However, little work of direct numerical analysis has been conducted on this subject because of the lack of effective computational methods for treating microcracks of a large number or of high concentration.

The effective field-subregion method presented in Section 2 is now adopted to calculate directly the Young's moduli of rectangular specimens containing up to thousands microcracks, as shown in Fig. 5(a). The average strain $\varepsilon_{ij}$ of a specimen subjected to uniform tensile stress $\sigma_{ij}^{\infty}$ on the boundary is amenable to an additive decomposition as

$$\varepsilon_{ij} = \varepsilon_{ij}^{0} + \varepsilon_{ij}^{c}, \tag{23}$$

where $\varepsilon_{ij}^{0}$ and $\varepsilon_{ij}^{c}$ denote the average strain tensor of the elastic matrix and its increase due to all the microcracks in the specimen, respectively. Assuming the matrix isotropic, $\varepsilon_{ij}^{0}$ and $\varepsilon_{ij}^{c}$ can be obtained by

$$\varepsilon_{ij}^{0} = M_{ijkl}\sigma_{kl}^{\infty} = \frac{1}{2E_0}[(1+v_0)(\delta_{ik}\delta_{jl}+\delta_{il}\delta_{jk}) - 2v_0\delta_{ij}\delta_{kl}]\sigma_{kl}^{\infty}, \tag{24}$$

$$\varepsilon_{ij}^{c} = \frac{1}{A}\sum_{\alpha=1}^{N} l_{\alpha}\left(\bar{b}_i^{(\alpha)} n_j^{(\alpha)} + \bar{b}_j^{(\alpha)} n_i^{(d)}\right), \tag{25}$$

respectively, where $\bar{b}_i^{(\alpha)}$ denotes the average opening displacement vector of the $\alpha$th microcrack. Once the pseudo-tractions on the $\alpha$th microcrack have been determined from the method in Section 2, its normal and tangential opening displacements can be given by

$$\bar{b}_1^{(\alpha)} = \frac{\pi l_\alpha}{E}[\cos\theta_\alpha\langle\tau^\alpha\rangle - \sin\theta_\alpha\langle p^\alpha\rangle],$$
$$\bar{b}_2^{(\beta)} = \frac{\pi l_\alpha}{E}[\sin\theta_\alpha\langle\tau^\alpha\rangle + \cos\theta_\alpha\langle p^\alpha\rangle]. \tag{26}$$

Thus, the average strains and thereby the effective moduli of a microcracked specimen can be determined. For the two cases of completely random orientation and aligned orientation of microcracks, the numerical results are shown in Figs. 8 and 9, respectively, in comparison with the experimental data of Carvalho and Labuz (1996), the numerical results of Kachanov (1993), as well as the analytical results obtained from the non-interacting approximation (or the dilute concentration method, DCM), SCM, DM, IDD and the method suggested by Feng and Yu (2000). Because each specimen has a very large number of microcracks (e.g., up to six thousands), no evident difference has been observed among the numerical results of different specimens with microcracks of the same distribution, as is contrary to the high dispersion of strength. As expected, the effective Young's modulus exhibits almost no size effect provided that the specimen is large enough to contain a sufficient number of microcracks. It is also found that the direct interaction of microcracks in the subregion also influences the effective elastic modulus evidently, that is, neglecting the interaction of microcracks in $\Omega$ may lead to a considerable error in effective elastic moduli. But in comparison with the SIFs, the effective elastic modulus shows a weaker dependence on the subregion dimension.

In addition, it is seen that the numerical estimates agree well with the experimental data of Carvalho and Labuz (1996), and the analytical results of the DM, IDD, and Feng and Yu's method. Especially, it is evident that the difference between the numerical calculation and the IDD prediction is very small even at very high concentration of microcracks. The estimates of DCM and SCM are satisfactory only when the scalar microcrack density is very small (e.g., less than 0.1). For comparison, Kachanov's calculation results (Kachanov, 1993) are also given in Figs. 8 and 9. For randomly oriented cracks, his solution agrees very well with the non-interacting approximation. For parallel cracks, his estimate for the effective Young's modulus is a little higher than the non-interacting solution. Kachanov (1993) attributed this slight stiffening effect to the dominance of the shielding effect of microcracks. Except under dilute concentrations, however, our present numerical solutions for effective elastic moduli are evidently lower than the non-interacting approximation in both the cases of microcrack orientations. The present scheme, though based partly on

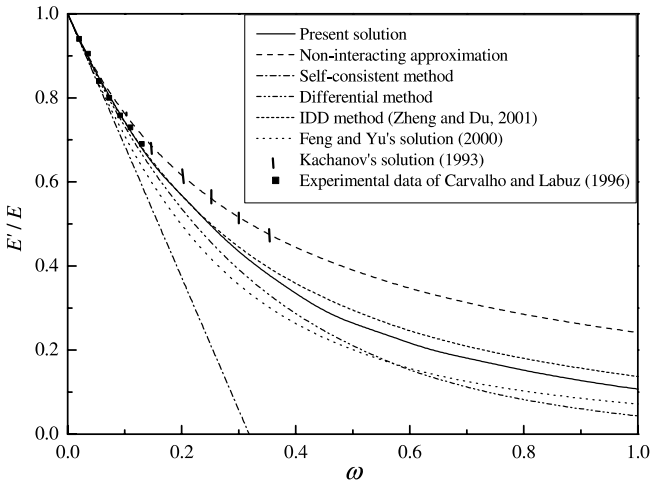


Fig. 8. Comparison of the effective Young's modulus of a 2D solid containing microcracks of completely random orientations.

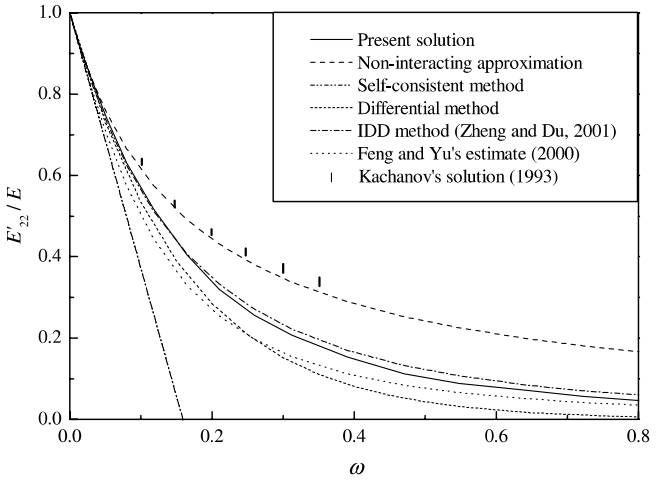


Fig. 9. Comparison of the effective Young's modulus of a 2D solid containing aligned microcracks.

the Kachanov method, leads to results at variance with those of Kachanov (1993). This is attributed to the contribution of the cracks in the complementary region $S - \Omega$. On one hand, further experimental evidence will be of great interest for examining the accuracy of these solutions. On the other hand, Zheng and Du (2001) proved in a strict way that the IDD method has a high accuracy even for high concentration of microcracks. This seems an indirect evidence for the good accuracy of the present solution. Therefore, the method presented in Section 2 provides a useful tool for evaluating various micromechanics methods for the effective elastic moduli of microcracked solids.

## 6. Conclusions

The deformation and failure behaviors of such brittle materials as ceramics and concrete are rather more than often associated with interacting microcracks. The effective elastic moduli of microcracked solids depend mainly on the statistically average effects of microcrack interaction, while the fracture and failure properties of materials are sensitive to higher-order effects of microcrack interaction. Therefore, it is of interest to assess quantitatively the effects of microcrack interaction from the viewpoint of micromechanics.

An approximate method is presented here to calculate the interaction of microcracks of a large number. To determine the SIFs of a microcrack, the microcracked solid is divided into two regions, which are dealt with in different ways. The interacting microcracks within an elliptical region around the considered microcrack are calculated directly by using Kachanov's interaction method, while the influence of other microcracks is reflected by modifying the far-field stress. This simplified scheme yields a satisfactorily accurate estimate of stress intensity factors.

This global/local method is first employed to analyze the size effect of strength of brittle specimens containing numerous microcracks. Both the cases of tension and compression are considered. As another example of its application, direct numerical calculations have been conducted for the effective elastic moduli of 2D microcracked solids in order to provide a valuable numerical reference for evaluation of various micromechanics methods. Some further potential applications of this method include the simulation of the failure process of microcrack-weakened materials, the transmission from distributed evolution of damage to damage localization, the behavior of microcrack clusters, and so on. Though the method is presented only for 2D problems in this paper, its 3D extension is of considerable interest.

**Acknowledgements**

X.-Q. Feng wishes to thank Prof. Quanshui Zheng and the two anonymous reviewers for their helpful comments. The authors acknowledge the support from the National Natural Science Foundation (Grant nos. 19891180 and 10028204) and the Education Ministry of China.

## Appendix A. Kachanov's method of microcrack interaction

For completeness, Kachanov's method of microcrack interaction is reviewed very briefly here. For more details, the reader is referred to Kachanov (1987, 1993). According to the superposition principle of elasticity, the problem of a linear elastic solid containing traction free cracks and subjected to a uniform stress $\boldsymbol{\sigma}_\infty$ on the boundary is equivalent to the problem where the traction stress $\mathbf{t}^\alpha_\infty = -\mathbf{n}^\alpha \cdot \boldsymbol{\sigma}_\infty$ is applied to the crack faces and the boundary of the solid is traction free, in the sense that they lead to identical results for the stress intensity factors of all microcracks. The latter problem is further considered as a superposition of $N$ subproblems each containing one crack subjected to pseudo-tractions as yet unknown. Accounting for microcrack interaction, thus, the tractions along the $\alpha$th crack are given by

$$\mathbf{t}^\alpha(\xi) = \mathbf{t}^\alpha_\infty + \mathbf{n}^\alpha \cdot \sum_{\beta\neq\alpha} \boldsymbol{\sigma}^{\alpha\beta}(\xi), \tag{A.1}$$

where $\boldsymbol{\sigma}^{\alpha\beta}(\xi)$ denotes the stress tensor induced by the $\beta$th crack at point $\xi$ along the $\alpha$th crack.

In the approximate method of Kachanov (1987), the key assumption that results in a major simplification of the problem is that the tractions in Eq. (A.1) are averaged over the $\alpha$th crack, and denoted as $\langle \mathbf{t}^\alpha \rangle$. This means that the impact of the traction fluctuation $\mathbf{t}^\alpha(\xi) - \langle \mathbf{t}^\alpha \rangle$ along the $\alpha$th crack on other cracks is neglected. This method leads to a satisfactory accuracy of the SIFs except in some cases, e.g., two microcracks perpendicular to each other and very small in spacing.

Let $\boldsymbol{\sigma}^{\alpha\beta}_n(\xi)$ and $\boldsymbol{\sigma}^{\alpha\beta}_\tau(\xi)$ denote the stresses generated at position $\xi$ along the $\alpha$th crack when the $\beta$th crack is subjected to a uniform normal traction and a uniform tangential traction of unit intensity, respectively. Thus, the normal and tangential pseudo-tractions on the $\alpha$th crack are simplified as

$$\begin{aligned} p^\alpha(\xi) &= p^\alpha_\infty + \mathbf{n}^\alpha \cdot \sum_{\beta\neq\alpha} [\boldsymbol{\sigma}^{\alpha\beta}_n(\xi)\langle p^\beta\rangle + \boldsymbol{\sigma}^{\alpha\beta}_\tau(\xi)\langle \tau^\beta\rangle] \cdot \mathbf{n}^\alpha, \\ \tau^\alpha(\xi) &= \tau^\alpha_\infty + \mathbf{n}^\alpha \cdot \sum_{\beta\neq\alpha} [\boldsymbol{\sigma}^{\alpha\beta}_n(\xi)\langle p^\beta\rangle + \boldsymbol{\sigma}^{\alpha\beta}_\tau(\xi)\langle \tau^\beta\rangle] \cdot \mathbf{m}^\alpha, \end{aligned} \tag{A.2}$$

respectively, where $\mathbf{m}^\alpha$ is the unit vector along the $\alpha$th crack (Fig. 2), the angle brackets stand for the average of a parameter over the crack surface.

Averaging Eq. (A.2) over the $\alpha$th crack, a system of $2N$ linear algebraic equations with respect to $\langle \mathbf{t}^\alpha \rangle = \langle p^\alpha \rangle \mathbf{n}^\alpha + \langle \tau^\alpha \rangle \mathbf{m}^\alpha$ can be obtained as

$$\begin{aligned} \langle p^\alpha \rangle &= p^\alpha_\infty + \sum_{\beta\neq\alpha} [\Lambda^{\alpha\beta}_{nn}\langle p^\beta\rangle + \Lambda^{\alpha\beta}_{\tau n}\langle \tau^\beta\rangle], \\ \langle \tau^\alpha \rangle &= \tau^\alpha_\infty + \sum_{\beta\neq\alpha} [\Lambda^{\alpha\beta}_{n\tau}\langle p^\beta\rangle + \Lambda^{\alpha\beta}_{\tau\tau}\langle \tau^\beta\rangle], \end{aligned} \tag{A.3}$$

where the transmission $\Lambda$-factors characterize the attenuation of the average normal and tangential tractions in transmission of stresses from one crack to another (Kachanov, 1987). After the average tractions

$\langle \mathbf{t}^{\alpha} \rangle$ have been solved from this system, the pseudo-tractions $\mathbf{t}^{\alpha}(\xi)$ can be determined from Eq. (A.2), and then the stress intensity factors of the interacting cracks can be determined from Eq. (12).

## References


Basista, M., Gross, D., 2000. A note on crack interactions under compression. Int. J. Fracture 102, L67–L72.

Benveniste, Y., 1986. On the Mori–Tanaka's method in cracked bodies. Mech. Res. Comm. 13 (2), 193–201.

Bristow, J.R., 1960. Microcracks and the static and dynamic elastic constants of anneals and heavily cold-worked metals. British J. Appl. Phys. 11 (1), 81–85.

Budiansky, B., O'Connell, R.J., 1976. Elastic moduli of a cracked solid. Int. J. Solids Struct. 12 (1), 81–95.

Bueckner, H.F., 1975. The weight function of the configuration of collinear cracks. Int. J. Fracture 11 (1), 71–83.

Carpinteri, A., Scavia, C., Yang, G.P., 1996. Microcrack propagation, coalescence and size effects in compression. Eng. Fracture Mech. 54 (3), 335–347.

Carvalho, F.C.S., Labuz, J.F., 1996. Experiments on effective elastic modulus of two-dimensional solids with cracks and holes. Int. J. Solids Struct. 33 (28), 4119–4130.

Chen, Y.Z., 1995. A survey of new integral equations in plane elasticity crack problems. Eng. Fracture Mech. 51 (1), 97–134.

Christensen, R.M., Lo, K.H., 1979. Solutions for effective shear properties in three phase sphere and cylinder models. J. Mech. Phys. Solids 27 (4), 315–330.

Chudnovsky, A., Dolgopolsky, A., Kachanov, M., 1987. Elastic interaction of a crack with a microcrack array, Part I and II. Int. J. Solids Struct. 23 (1), 1–21.

Feng, X.Q., 2001. On estimation methods for effective moduli of microcracked solids. Arch. Appl. Mech. 71 (8), 537–548.

Feng, X.Q., Yu, S.W., 2000. Estimate of effective elastic moduli with microcrack interaction effects. Theor. Appl. Fracture Mech. 34 (3), 225–233.

Feng, X.Q., Yu, S.W., 2002. Damage Micromechanics of Quasi-Brittle Materials (in Chinese). Higher Education Press, Beijing.

Gong, S.X., Horii, H., 1989. General solutions to the problems of microcracks near the tip of a main crack. J. Mech. Phys. Solids 37 (1), 27–46.

Hashin, Z., 1988. The differential scheme and its application to cracked materials. J. Mech. Phys. Solids 36, 719–734.

Hori, M., Nemat-Nasser, S., 1987. Interacting microcracks near the tip in the process zone of a macro-crack. J. Mech. Phys. Solids 35, 601–629.

Horii, H., Nemat-Nasser, S., 1983. Overall moduli of solids with microcracks: load-induced anisotropy. J. Mech. Phys. Solids 31 (2), 155–171.

Huang, Y., Chandra, A., Jiang, Z.Q., et al., 1996. The numerical calculation of two-dimensional effective moduli for microcracked solids. Int. J. Solids Struct. 33 (11), 1575–1586.

Huang, Y., Hu, K.X., Chandra, A., 1994. A generalized self-consistent mechanics method for microcracked solids. J. Mech. Phys. Solids 42 (8), 1273–1291.

Kachanov, M., 1987. Elastic solids with many cracks: a simple method of analysis. Int. J. Solids Struct. 23 (1), 23–43.

Kachanov, M., 1993. Elastic solids with many cracks and related problems. Advances in Applied Mechanics 30, 259–445.

Kanninen, M.F., Popelar, C.P., 1985. Advanced Fracture Mechanics. Oxford University Press, London.

Karihaloo, B.L., 1979. Fracture of solids containing arrays of cracks. Eng. Fracture Mech. 12 (1), 49–77.

Krajcinovic, D., 1996. Damage Mechanics. Elsevier, Amsterdam.

Lehner, F.K., Kachanov, M., 1995. On the stress–strain relations for cracked elastic materials in compression. In: Rossmanith, H.P. (Ed.), Mechanics of Jointed and Faulted Rock. Balkema, The Netherlands, pp. 49–61.

Mori, T., Tanaka, K., 1973. Average stress in matrix and average elastic energy of materials with misfitting inclusions. Acta Metall. 21, 571–574.

Mura, T., 1987. Micromechanics of Defects in Solids. Martinus Nijhoff Publishers, The Netherlands.

Nemat-Nasser, S., Hori, M., 1993. Micromechanics: Overall Properties of Heterogeneous Materials. North-Holland, Amsterdam.

Petrova, V., Tamuzs, V., Romalis, N., 2000. A survey of macro-microcrack interaction problems. Appl. Mech. Rev. 53 (5), 117–146.

Shen, L.X., Yi, S., 2001. An effective inclusion model for effective moduli of heterogeneous materials with ellipsoidal inhomogeneities. Int. J. Solids Struct. 38, 5789–5805.

Seelig, Th., Rafiee, S., Gross, D., 2000. A simple method for the investigation of elastic bodies of finite size containing many cracks. Int. J. Eng. Sci. 38 (13), 1459–1472.

Tada, H., 1973. The Stress Analysis of Cracks Handbook. Del Research Corporation, Paris.

Walpole, L.J., 1969. On the overall elastic moduli of composite materials. J. Mech. Phys. Solids 17, 235–251.

Yu, S.W., Feng, X.Q., 1995. A micromechanics-based model for microcrack-weakened brittle solids. Mech. Mater. 20, 59–76.

Yu, S.W., Feng, X.Q., 1997. Damage Mechanics (in Chinese). Tsinghua University Press, Beijing.

Zhan, S., Wang, T.C., Han, X.L., 1999. Analysis of two-dimensional finite solids with microcracks. Int. J. Solids Struct. 36 (25), 3735–3753.

Zheng, Q.S., Du, D.X., 1997. Closed-form interacting solutions for overall elastic moduli of composite materials with multi-phase inclusions, holes and microcracks. Key Eng. Mater. 145–149, 479–486.

Zheng, Q.S., Du, D.X., 2001. An explicit and universally applicable estimate for the effective properties of multiphase composites which accounts for inclusion distribution. J. Mech. Phys. Solids 49 (11), 2765–2788.

Zimmerman, R.W., 1985. The effect of microcracks on the elastic moduli of brittle materials. J. Mater. Sci. Lett. 4, 1457–1460.